European Polymer Journal 207 (2024) 112811

Contents lists available at ScienceDirect

European Polymer Journal

journal homepage: www.elsevier.com/locate/europolj

Cyclic polyglycolides via ring-expansion polymerization with cyclic tin catalysts

Steffen M. Weidner [a], Andreas Meyer [b], Hans R. Kricheldorf [c,*]

[a] BAM, Federal Institute of Materials Research and Testing, Richard Willstätter Str. 11, D-12489 Berlin, Germany
[b] Universität Hamburg, Institut für Physikalische Chemie, Grindelallee 117, D-20147 Hamburg
[c] Universität Hamburg, Institut für Technische und Makromolekulare Chemie, Bundesstr. 45, D-20146 Hamburg, Germany

ARTICLE INFO

Keywords:
Polyglycolides
Ring-expansion polymerization
MALDI-TOF-mass spectrometry
Crystallinity

ABSTRACT

Glycolide was polymerized in bulk with two cyclic catalysts – 2,2-dibutyl-2-stanna-1,3-dithiolane (DSTL) and 2-stanna-1,3-dioxa-4,5,6,7-dibenzepane (SnBiph). The monomer/initiator ratio, temperature (140 – 180 °C) and time (1—4 days) were varied. The MALDI TOF mass spectra exclusively displayed peaks of cyclic polyglycolide (PGA) and revealed an unusual "saw-tooth pattern" in the mass range below *m/z* 2 500 suggesting formation of extended ring crystallites. The DSC measurements indicated increasing crystallinity with higher temperature and longer time, and after annealing for 4 d at 160 °C a hitherto unknown and unexpected glass transition was found in the temperature range of 170–185 °C. Linear PGAs prepared by means of metal alkoxides under identical conditions did not show the afore-mentioned features of the cyclic PGAs, neither in the mass spectra nor in the DSC measurements. All PGAs were also characterized by SAXS measurements, which revealed relatively small L-values suggesting formation of thin crystallites in all cases with little influence of the reaction conditions.

1. Introduction

Soon after World War II a small-scale technical production of glycolide was established in the USA, and the commercial availability of this monomer stimulated research on synthesis and properties of polyglycolic acid (PGA). First patents in this direction were filed by members of DuPont and American Cyanamide in the early 1950ties [1–3], and after 1960 a slow but steady flow of academic papers and patents dealing with PGA followed. [4–29] The interest in synthesis, characterization and application of this polyester raised, when American Cyanamide reported on the usefulness of PGA as resorbable medical suture [4–6], which was commercialized after 1968 under the trademark "Dexon". A copolymer containing a small fraction of L-lactic acid (typically < 10 %) to improve flexibility and meltability was commercialized as "Vicryl" by Ethicon Inc. (Johnson & Johnson) in the early 1970ties. Both PGA fibers still serve as standard medical sutures in the 21st century. In addition to the ring-opening polymerization (ROP) of glycolide, two synthetic methods based on polycondensation processes were explored after 1984. [24–29].

PGA possesses a couple of interesting and extraordinary properties. Due to the lack of substituents and due to the high polarity of the repeat units PGA allows for a rather dense chain packing which entails, in turn, the following properties. PGA forms a highly stable crystal lattice with high melting temperatures (T_m values up to 230 °C), high melting enthalpies (measured ΔH_m up to 170 Jg^{-1}), high density (up to 1.69 g cm^{-1}), high hardness and excellent barrier properties. Despite these interesting and useful properties applications and research activities dealing with neat PGA were relatively scarce when compared with poly (L-lactide). The following negative properties of PGA are responsible for this situation. First, the polymerization is highly exothermic and the heat flow difficult to control when large quantities are polymerized. Second, processing from the melt requires temperatures above 230 °C which entails thermal degradation. Third, an inexpensive inert solvent allowing for processing from solution has not been found yet (for a detailed discussion of the solubility see text below). Fourth, PGA is more sensitive to hydrolysis than any other technically produced polyester, and the rapid hydrolytic degradation may be too fast for certain applications.

Nonetheless, PGA has recently found broader application in the form of films under the trademark "Kuradex", because these films combine high mechanical strength with excellent barrier properties, and thus, are useful for a variety of packing applications. The easier to process copolymers of glycolide containing lactide, ε-caprolactone or trimethylene carbonate have attracted a great scientific interest with the consequence

* Corresponding author.
E-mail address: hrkricheld@aol.de (H.R. Kricheldorf).

https://doi.org/10.1016/j.eurpolymj.2024.112811
Received 6 December 2023; Received in revised form 25 January 2024; Accepted 28 January 2024
Available online 6 February 2024

of numerous publications and patents, because of their usefulness as drug-delivery systems.

In the case of poly(L-lactide), PLA, interest in cyclic PLAs has rapidly increased over the past 15 years, because their properties may be advantageous over those of the linear counterparts. In this connection the authors have found interesting new phenomena concerning crystallization of cyclic PLAs. These findings have now stimulated the authors to study synthesis and characterization cyclic PGAs. In this first report, ring-expansion polymerization (REP) by means of cyclic tin catalysts was used as synthetic approach (Scheme 1). Two catalysts, DSTL[30] and SnBiph[31] (for definition see Scheme 1) were used for two reasons. First, numerous medium and high molar mass cyclic polylactides were prepared with theses catalyst under various reaction conditions.[30–34] Second, both Sn compounds proved to be active transesterification catalysts in solid PLAs.[32–35].

2. Experimental

2.1. Materials

Glycolide was purchased from Physcience (Hirschberg, Germany) and recrystallized from anhydrous tetrahydrofuran (THF)/toluene mixtures. Anhydrous THF and toluene were purchased from Fisher Scientific (Schwerte, Germany). Hexafluoro-*iso*-propanol (HFIP), titanium tetra butoxide, zirconium tetra butoxide and aluminum *iso*-propoxide were purchased from Alfa Aesar (Kandel, Germany and used as received. 1,4-butane diol was purchased from Sigma-Aldrich, dried azeotropically with toluene and stored over mol-sieves. The catalysts 2.2-dibutyl-2-stanna-1,3-dithiolane (DSTL)[30], 2-stanna-1,3-dioca-4,5,6,7-dibenzepane (SnBiph)[31] and dibutyltin bisbenzyloxide[30] were prepared as described previously.

2.2. Reps with neat catalysts (Tables 1 and 2)

The catalyst (0.08 mmol) and glycolide (40 mmol) were weighed into a 50 mL flame-dried Erlenmeyer flask under a blanket of argon, and a magnetic bar was added. The reaction vessel was immersed into an oil bath thermostated at 140, 160 or 180 °C. After cooling of the resulting PGA to ca. 25 °C the reaction vessel was destroyed and the solid disk of PGA was cracked into 4–6 pieces, which were used for annealing or direct characterization.

2.3. Rops initiated with metal alkoxides (Table 3)

Dibutyltin dibenzyl oxide (0.4 mmol), titanium or zirconium tetra butoxide (0.2 mmol), and glycolide (40 mmol) were weighed into a flame dried 50 mL Erlenmeyer flask under a blanket of argon and a magnetic bar was added. The closed reaction vessel was immersed into an oil bath thermostated at 140 °C. The cold PGA disks were cracked with a spatula (they were more brittle than those of the cyclic PGAs). Approximately 50 % of the product was used for characterization and the other 50 % for annealing at 140 °C under an atmosphere of argon.

For the polymerization with aluminum *iso*-propoxide 0.3 mmol of the catalyst and 45 mmol of glycolide were used.

2.4. Measurements

The MALDI TOF mass spectra were measured with Autoflex maX mass spectrometer (Bruker Daltonik GmbH, Bremen, Germany) equipped with a Smartbeam laser ($\lambda = 355$ nm). All spectra were recorded in the positive ion linear mode. The MALDI stainless steel targets were prepared from solutions of PGA in HFIP and doped with potassium trifluoroacetate (2 mg mL^{-1}). Typically, 20 μL of sample the solution, 2 μL of the potassium salt solution and 50 μL of a solution of *trans*-2-[3-(4-*tert*-butylphenyl)-2-methyl-2-propenylidene] malononitrile (DCTB, 20 mg

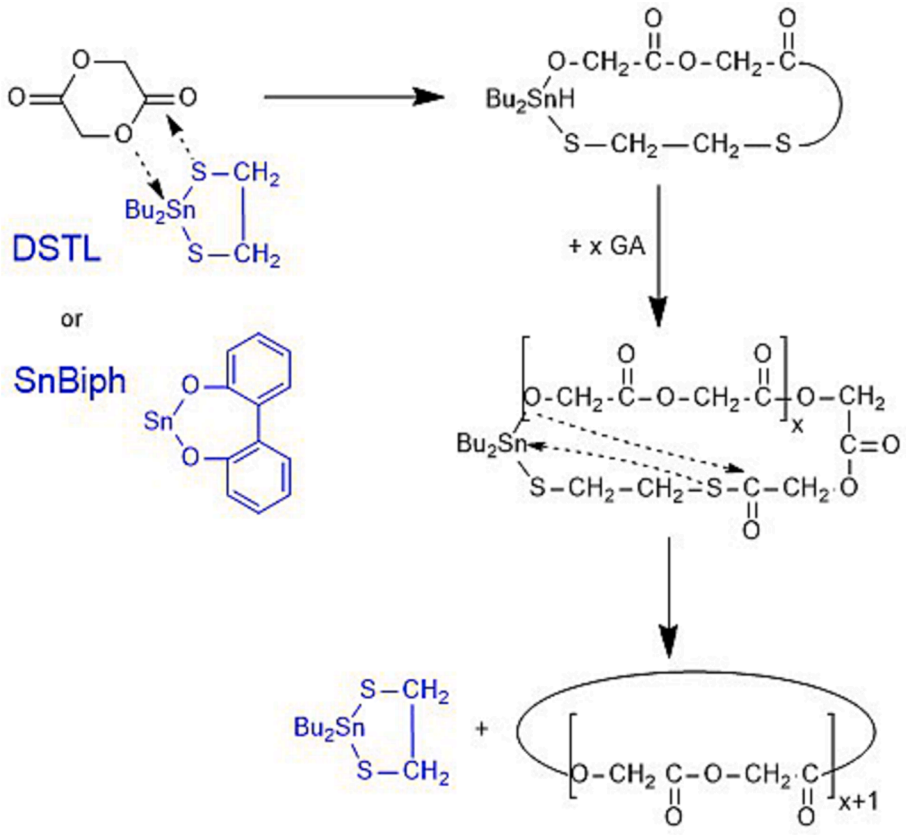

Scheme 1. Structure of used catalysts (blue) and mechanism of ring-expansion polymerization (REP) of glycolide catalyzed by DSTL.

mL^{-1} in $CHCl_3$) serving as matrix were mixed in an Eppendorf vial. 1 μL of the corresponding solution was deposited on the MALDI target. Manufacturer software FlexControl was used to record spectra by accumulating 2000 single laser shots recorded at 4 different positions. Molecular weight calculations were performed using a freeware program (Molecular Weight Calculator, https://ncrr.pnl.gov/software/). Since all measurements were performed in linear modus, average masses were used for calculation.

The GPC measurements were performed in a modular system kept at 30 °C consisting of an isocratic pump (Agilent, USA) running with a flow rate of 0.5 mL min^{-1} and a refractive index detector (RI-501-Shodex). HFIP was used as eluent. Samples were manually injected (100 μL, ca. 2–4 mg mL^{-1}). For instrument control and data calculation WinGPC software (Polymer Standard Service-PSS now Agilent, Mainz, Germany) was used. The calibration was performed using polymethylmethacrylate (PMMA) standards (Polymer Standards Service – PSS, Mainz).

The DSC heating traces were recorded on a (with indium and zinc freshly calibrated) Mettler-Toledo DSC-1 equipped with Stare Software-11 using a heating rate of 10 K min^{-1}. Only the first heating traces were evaluated. The crystallinities were calculated using a ΔH_m max of −206 J g^{-1}, which was mentioned and used by Ramdanhie et al. [15] and Ayyoob et al. [21] as the value published by the manufacturer of the Dexon fiber.

The SAXS measurements were performed using our in-house SAXS/WAXS apparatus equipped with an Incoatec™ X ray source IμS and Quazar Montel optics. The wavelength of the X ray beam was 0.154 nm and the focal spot size at the sample position was 0.6 mm^2. The samples were measured in transmission geometry and were recorded with a Rayonix™ SX165 CCD-Detector. The SAXS measurements were performed at sample-detector distance of 1.6 m and the accumulation was 1200 s for each position. DPDAK, a customizable software for reduction and analysis of X-ray scattering data sets was used for gathering 1D scattering curves.[36] For the evaluation of the crystallinity of the samples the data were imported in Origin™ and analyzed with the curve fitting module. The SAXS curves were converted into Kratky plots. The long periods of the lamellar domains were determined by the q values of the reflection maxima.

3. Results and discussion

3.1. Solubility and GPC measurements

Reports on the solubility of PGA are inconsistent and confusing. Therefore, the authors considered it useful to present a detailed discussion of the solubilities reported in the literature and those found for their own samples. In numerous research papers and review articles [9,10,13,17,18,25,27–29] PGA is mentioned to be soluble in hexafluoro-*iso*-propanol (HFIP), and GPC measurements were conducted by several research groups using this solvent. These reports have in common that with one exception[13], the PGAs under investigation, had a linear topology due to initiation with an alcohol. Furthermore, several research groups mentioned, that according to a Handbook[37], the solubility of PGA is limited to molar masses < 45 000 g mol^{-1} (apparently the number average was meant). Finally, the work of Dobrzynski et al.[13] needs discussion. Those authors polymerized GL with neat anhydrous calcium acetylacetonate in bulk. They found that only the low molar mass PGA isolated at conversions < 30 % was soluble in HFIP. Unfortunately, the topology of these PGAs is not clear, because in the absence of an initiator cyclic PGAs might have been formed. Those authors did not suspect formation of cyclic PGAs and did not characterize their samples by MALDI TOF mass spectrometry. Furthermore, no detailed study of metal acetylacetonate-catalyzed polymerizations of lactide has been published (to the best knowledge of the authors), so that any source of information concerning the topology of the PGAs prepared by Dobrzynski et al. is missing.[13] This aspect is of interest, in connection with the results found in this work.

When compact fragments of the PGA disks prepared by cyclic catalysts in the present work were stirred with HFIP at 22 °C for 2 days, no dissolution was detectable. When the samples listed in Tables 1 and 2 were powdered, stirred in HFIP at 40 °C and irradiated with ultrasound parts of the samples went in solution, but (almost) complete solution was achieved only in less than 50 % of all samples. In these cases, GPC measurements were performed. The linear PGAs isolated after a short time were completely soluble in HFIP, but after annealing only a fraction of these PGAs was soluble. It was also observed for cyclic PGAs that annealing reduces the solubility apparently due to increasing crystallinity and perfection of crystallites. Number average (M_n) and weight average molar masses (M_w) were only measured, when a sample was completely soluble or slightly turbid (measured after filtration).

In Fig. 1A the elution curve of a low molar mass sample (No. 1A, Table 1) which displays a bimodal distribution with high dispersity is presented. All other samples yielded monomodal elution curves with weak shoulders such as that displayed in Fig. 1B. Extremely high M_n and M_w values were found for most PGAs of Table 1 and 2. These molar masses were higher than all M_n and M_w values reported in the literature so far. However, for REPs of L-lactide with DSTL M_n up to 200 000 and M_w up to 400 000, and with SnBiph M_n up to 150 000 and M_w up to 425 000 were also achieved.[34].

3.2. MALDI-TOF mass spectrometry

The polymerizations performed with DSTL were summarized in Table 1 and those conducted with SnBiph in Table 2. Relatively high catalysts concentrations were chosen, to ease the detection of catalytic activities upon annealing of the PGAs in the solid state. Temperature and time were varied in both series. The MALDI TOF mass spectra of all samples listed in Tables 1 and 2 have in common that the signal-to-noise ratio was poor when compared with mass spectra of PLA. This finding is mainly a result of the stable crystal lattice of PGA based on a dense packing of antiparallel chain segments, which favours strong electronic interactions, because dipole–dipole interactions and van der Waals forces increase with the seventh power when the distance decreases. All mass spectra displayed peaks of cycles and in the best spectra these peaks were observable up to *m/z* 7 000 corresponding to a degree of polymerization around 120 (Fig. 2B and 3B). These mass spectra are not representative for the high molar mass fraction of the PGAs, but the polymerization mechanism does not involve a formation of linear chains, so that a cyclic topology of polymers is the only possible topology. A few linear chains might have been formed by side reactions, but an analytical tool allowing for the detection of a few percent of linear chains in a high molar mass sample of a cyclic polymer does not exist. The comparison of intrinsic viscosities with absolute molecular masses is not accurate enough for this purpose.

The most conspicuous feature of the mass spectra of the samples prepared with DSTL at 180 °C is the high intensity of cycles having degrees of polymerization (DPs) of 28, 32 and 36 Fig. 2A). More informative mass spectra with a broader mass range and better signal-to-noise ratio were obtained at 160 °C and 140 °C and the best example is displayed in Fig. 2B.

Typical “saw-tooth patterns” (STP) were now detectable with a distance of 4 repeat units between the tips of the “tooth”.

SnBiph catalyzed PGAs showed a poor signal-to-noise ratio when polymerized at 200 °C, possibly due to a high molecular weight. Nonetheless, a weak STP was still detectable (Fig. 3A). At 180 °C/1d (2A, Table 2) the mass spectrum was almost identical with that presented in Fig. 2A. Samples polymerized at 160 or 140 °C showed STPs analogous to those found for DSTL catalyzed PGAs (Fig. 3B and Figures S1 and S2, suppl., part). These STPs are characterized by a periodicity of four repeat units and the most prominent peaks are always even-numbered cycles: C16 (not displayed in the Figures), C20, C24, C28, C32 and C36. These tips are identical for all samples and thus, indicate that they were formed under thermodynamic control. In other

Table 1
REPs catalyzed with DSTL in bulk: variation of temperature and time.

Exp. No.	GL/Cat	Temp. (°C)	Time(d)	T_g	T_m(°C)	M_n	M_w	Đ	ΔH_m (Jg^{-1})	Cryst. (%)[a)]	L (nm)	l_c [b)](nm)
1A	500/1	180	1	–	212.7	29 000	40 000	1.38	138.0	66	7.7	5.0
1B	500/1	180	2	–	214.7	–	–	–	119.3	58	–	–
2A	500/1	160	1	–	224.0	–	–	–	122.7	59	7.6	4.4
2B	500/1	160	4	–	226.1	382 000	678 000	1.77	131.6	64	7.4	4.8
3A	100/1	160	1	–	224.3	–	–	–	116.5	57	7.6	4.3
3B	100/1	160	4	–	224.4	220 000	422 000	1.92	126.5	62	7.3	4.5
4A	100/1	140	1	–	225.5	305 000	490 000	1.61	109.7	53	7.5	4.0
4B	100/1	140	4	170.0	223.2	–	–	–	111.0	54	7.2	3.9

a) calculated from DSC measurements with a ΔH_m^0 of 206 Jg^{-1}, b) thickness of crystallites estimated by multiplication of L with the crystallinity.

Table 2
REPs catalyzed with SnBiph (GL/Cat = 500/1) in bulk: variation of temperature and time.

Exp. No.	Temp. (°C)	Time(d)	T_g(°C)	T_m(°C)	M_n	M_w	Đ	ΔH_m (Jg^{-1})	Cryst. (%)[a)]	L(nm)	l_c [b)](nm)
1A	200	2 h	–	222.3	–	–	–	117.3	57	8.1	4.6
1B	200	1	–	228.9	–	–	–	132.0	64	7.8	5.0
1C	200	3	–	232.1	–	–	–	143.2	69	7.2	4.9
2A	180	1	–	215.4	3 200	4 000	1.25	140.3	67	7.4	4.8
2B	180	3	–	225.7	286 000	460 000	1.61	153.8	75	7.7	5.7
2C	180	6	–	227 + 233	–	–	–	157.6	77	6.7	5.2
3A	160	1	–	222.4	360 000	610 000	1.69	119.1	58	7.3	4.2
3B	160	4	180.5	223.5	220 000	440 000	2.00	127.6	62	7.1	4.3
4A	140	1	–	224.0	–	–	–	95.5	46	7.2	3.3
4B	140	4	180.6	224.8	2 700[c)]	15 000	5.56	108.0	52	7.6	4.0

a) calculated with a ΔH_m^0 of 206 Jg^{-1}, b) thickness of crystallites estimated by multiplication of L with the crystallinity, c) bimodal elution curve.

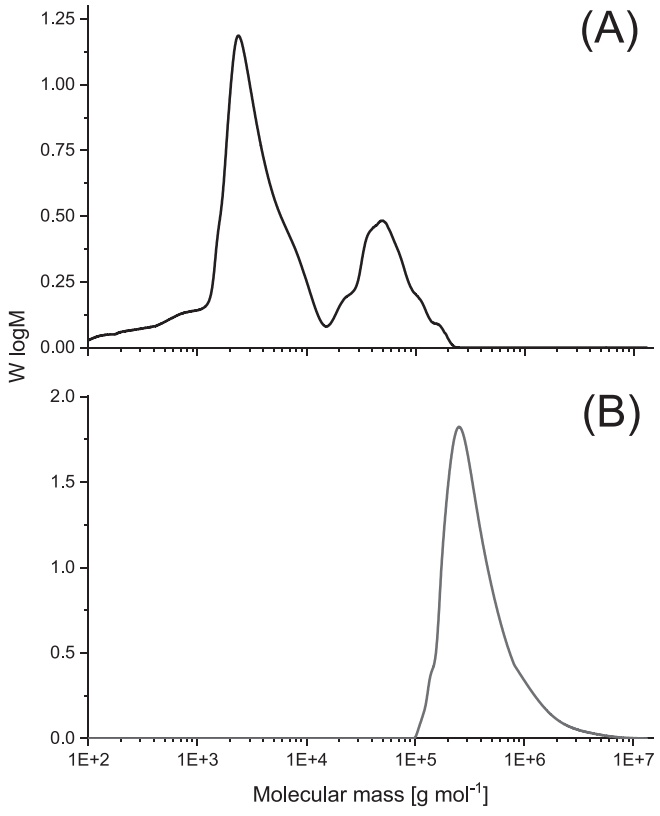

Fig. 1. GPC elution curves of DSTL-catalyzed PGAs: (A) 180 °C/1 d (1A, Table 1), (B) 140 °C/1 d (4A, Table 1).

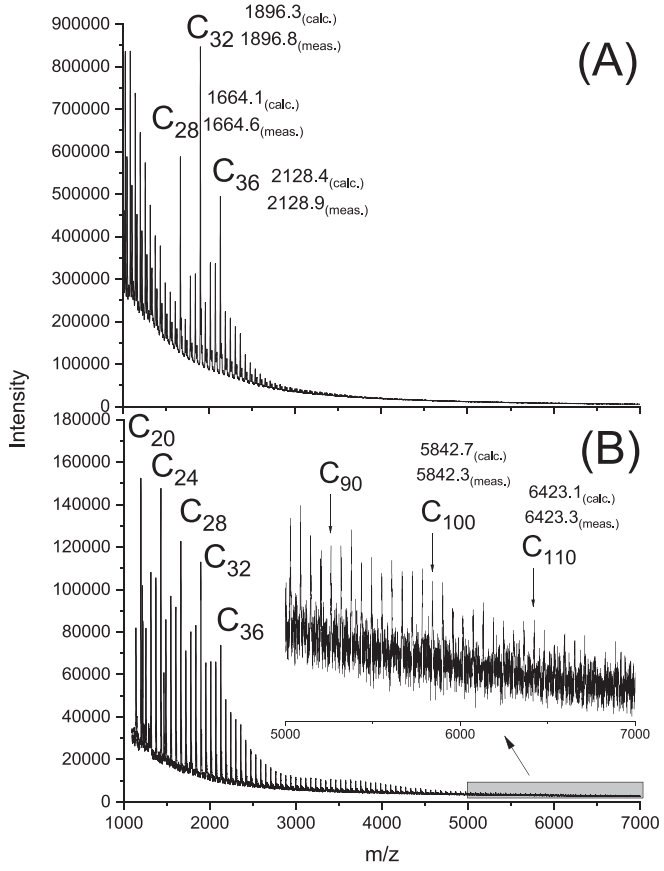

Fig. 2. MALDI TOF mass spectra of PGAs prepared with DSTL: (A) at 180 °C/1 d (1A, Table 1), (B) at 160 °C/4 d (3B, Table 1).

words, the predominance of even-numbered cycles below *m/z* 2 500 did not results from a kinetically controlled polymerization in the melt, but from a thermodynamically controlled transesterification across the

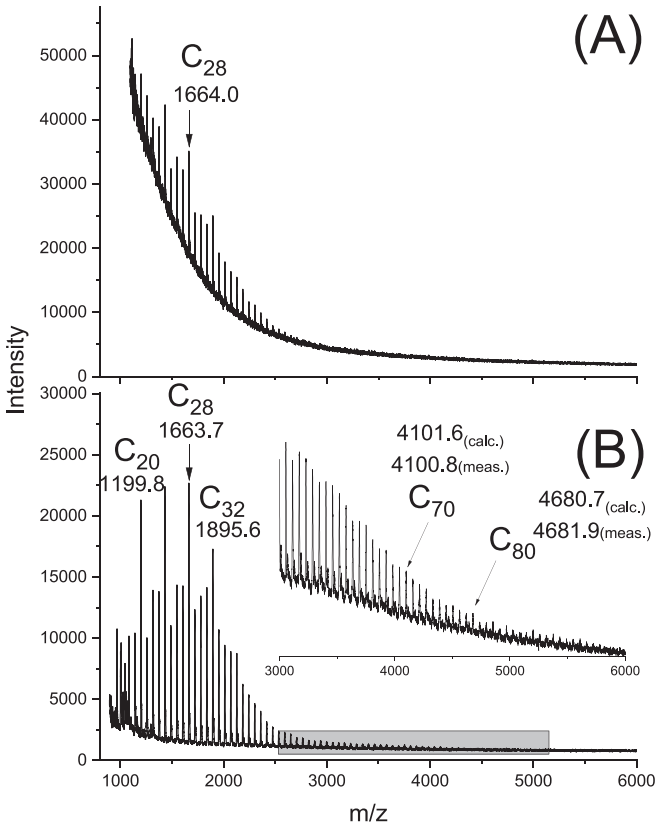

Fig. 3. MALDI TOF mass spectra of PGAs prepared with SnBiph: (A) at 200 °C/2h (1A, Table 2), (B) at 160 °C/4 d (3B, Table 2).

surface of the crystallites. A reaction mechanism explaining expansion and contraction of loops on the surface of crystallites is outlined in Scheme 2.

For a proper interpretation of this phenomenon, it was essential to check, if the mass spectra of linear PGAS annealed at 140 °C also display a STP. Initial attempts to prepare linear PGAs by alcohol-initiated ROPs catalyzed by DSTL, SnBiph or $SnOct_2$ at 140 °C failed, because in addition to expected linear chains large amounts of cycles were formed. A detailed study of such ROPs will be published elsewhere. Therefore, an

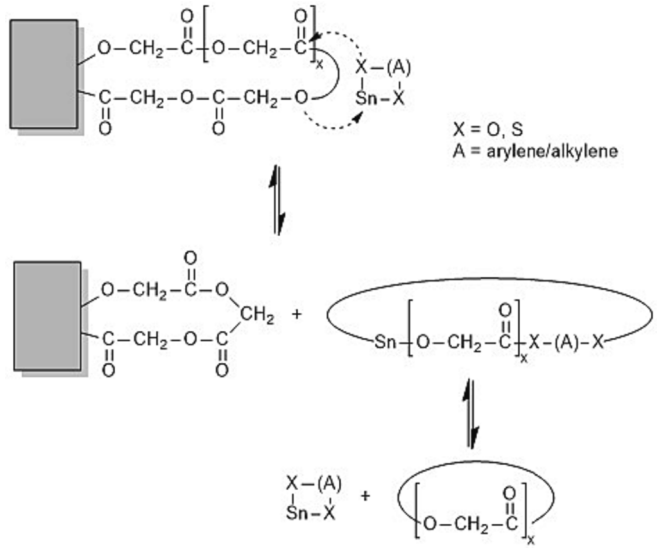

Scheme 2. Contraction and expansion of loops on the surface of crystallites via transesterification with cyclic tin catalysts.

alternative approach, namely metal alkoxides-initiated ROPs were conducted, and the resulting PGAs were annealed for 4d at 140 °C (Table 3). The mass spectra of these four PGAs displayed indeed the expected peaks of linear chains almost free of cycles (Fig. 4).

STPs were observed in the mass spectra of cyclic PLAs for the first time [32,34,35,38], but those PLA patterns differ from the STPs of PGAs in three aspects. First, the teeth in the PLA mass spectra were symmetrical. Second, they covered a periodicity of six repeat units. Third, the STPs typically covered a mass range of *m/z* 4 000—12 000[34,38] and extended in favorable cases up to *m/z* 15 000. A typical example prepared with SnBiph is displayed in Figure S3.

The interpretation of these STPs is based on the following experimental results:

1. STPs were never observed for linear PLAs regardless of initiator, catalyst, temperature and time.[30,39]
2. STPs were never observed for cyclic PLAs isolated from the melt. [30,35,39–41]
3. Formation of the STP requires annealing times of 1d or more
4. The STP appears in combination with a new broad maximum of the mass distribution around *m/z* 8 000.[32,34,35,38]
5. The length of extended-ring in the mass range of *m/z* 4 000 – 15 000 fits in with the crystal thickness found by SAXS for annealed cyclic PLAs.[38]

The conspicuous difference between the mass range observed for PGAs, on the one hand, and PLAs, on the other, can be understood by considering the low thickness of the PGA crystallites and the lower mass of the repeat units. As demonstrated in Tables 1 and 2 and discussed below, the typical long-distance value (L) of PGA falls into the range of 7.1–7.8 nm, and thus, is by factor of 4–5 smaller than that of annealed cyclic PLAs.[32,][38] Furthermore, the mass of glycolyl unit is about 20 % lower than the mass of a lactyl unit. Hence, the mass range of the PLAs must be divided by a factor of 6 to yield the mass range, where PGAs may form STPs. From the maximum mass range of PLA (*m/z* 4 000–15 000) a range of *m/z* 700–2 500 may be calculated for PGA and from the narrower mass range (*m/z* 5 000–12 000) typical for most PLAs, the calculated mass range of PGA amounts to *m/z* 800–2 000 in perfect agreement with the mass range observed in the mass spectra of the PGAs (Fig. 2B and 3B).

When the length of extended PGA rings is compared with the crystal thickness as indicated by SAXS measurements, the following conclusions may be drawn. Assuming that at least one repeat unit is required to form a loop, then the maximum length of C28 amounts to 13 glycolyl units and the maximum length of C36 is 16 repeat units. For the length of 10 glycolyl units in crystalline PGA values of 3.01 and 3.02 nm were reported[6,42] Hence, an extended C28 ring has a length of approximately 4.0 nm and C36 has a maximum length of the linear segments of 16 glycolyl units corresponding to 5.1–5.2 nm. A rough estimation of the crystallite thickness (l_c) may be deduced from the L-values by multiplication with the crystallinity determined by DSC. The l_c values obtained in this way (Tables 1 and 2) perfectly agree with the calculated length of PGA cycles, and thus, support the hypothesis that the PGA rings form extended-ring crystals.

The question why low molar mass cycles of PGA and PLA form extended-ring crystals has been discussed for PLAs in several recent publications[35,43,44] but the main arguments should be repeated here again. These crystals represent the thermodynamically most favorable kind of crystallites for the following reasons. First, extended rings automatically crystallize with a perfect 1:1 ratio of antiparallel chains, the energetic optimum reported for the most stable modification of PGA and PLA (Fig. 5A).This optimum does not necessarily result from a kinetically controlled crystallization of linear chains as illustrated in Fig. 5B. In the case of linear chains, kinetically controlled crystallization may result in a few parallel chain alignments and end groups may be buried inside the crystallites. Second, crystallites formed by cycles with

Table 3
Syntheses of linear PGAs in bulk at 140 °C with variation of the initiator.

Exp. No.	Initiator (Catalyst)	GL/In	Time (d)	M_n	M_w	Đ	T_m(°C)	ΔH_m (Jg^{-1})	Cryst. (%)[a)]
1A	$Bu_2Sn(OBn)_2$	100/1	1	7 800	8 900	1.14	223.6	102.2	49
1B			4	–	–	–	220.0	123.2	59
2A	$Al(OiPr)_3$	150/1	1	-[b)]	–	–	–	–	–
2B			4	–	–	–	220.2	98.0	47
3A	$Ti(OBu)_4$	200/1	1	7 200	8 200	1.14	225.0	100.0	48
3B			4	–	–	–	223.3	98.7	47
4A	$Zr(OBu)_4$	200/1	1	7 400	7 900	1.07	223.2	98.3	47
4B			4	–	–	–	223.0	98.7	47

a)calculated with a ΔH_m^0 of 206 Jg^{-1}, b) no polymerization

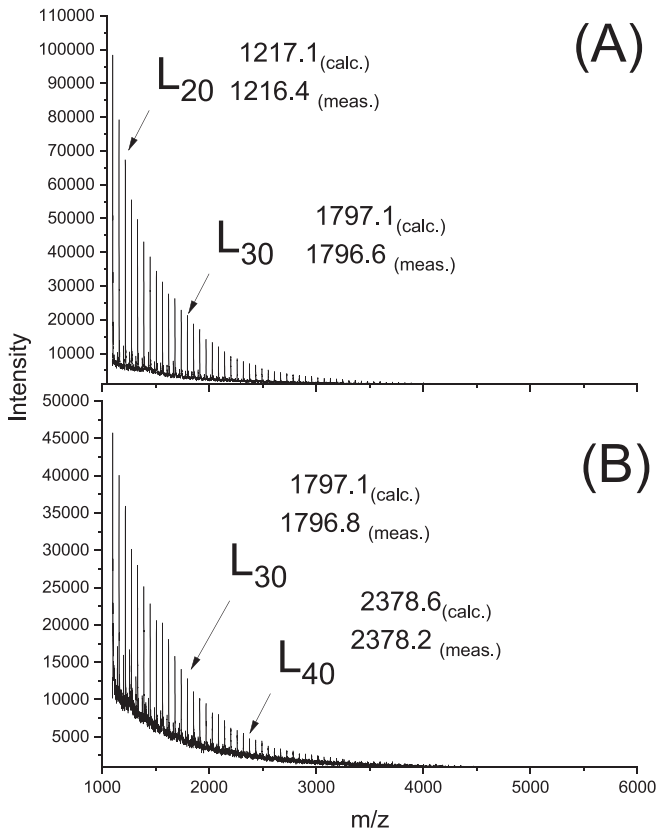

Fig. 4. MALDI.TOF mass spectra of PGAs prepared at 140 °C (A) with $Ti(OBu)_4$ (3A, Table 3), (B) with $Zr(OBu)_4$ (4B, Table 3).

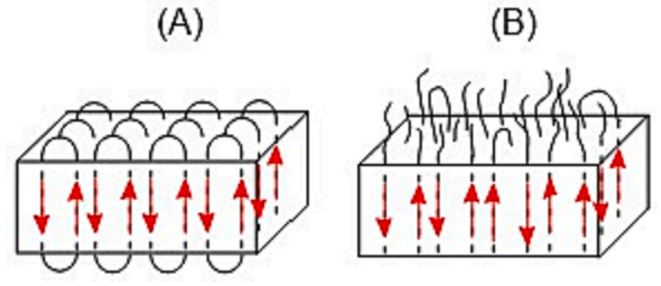

Fig. 5. Schemes of extended-ring crystals (A) and linear chain crystals (B).

low dispersity do not contain defects resulting from a burial of end groups inside the crystal lattice in contrast to crystallites of linear chains (Fig. 5B). Third, crystallites of extended rings with low dispersities possess a relatively uniform and smooth surface with a perfect parallel alignment of loops of similar size, whereas the surface of crystallized linear chains is more complex (Fig. 5B). The formation of a STP represents a further optimization of the crystal surface, because it indicates that each crystallite is built up by cycles with narrow size distribution. Each tooth represents a group of crystallites defined by the same ring size and dispersity. The tip of the tooth indicates the most abundant ring size in each group of crystallites. Why the periodicity of the teeth in PGA is four, but six in the case of PLA cannot be answered at this time.

3.3. DSC measurements

All DSC measurements (Figs. 6 and 7) were performed with a heating rate of 10 K min^{-1} in analogy to almost all DSC measurements reported in the literature. The DSC heating curves of all cyclic PGAs displayed only weak glass transition step in the temperature range of 37–45 °C and a strong monomodal melting endotherm. Concerning T_m and ΔH_m the following trends were observed in both series of REPs (Tables 1 and 2). First, in the temperature range of 140–180 °C, the T_m increases with lower temperature when compared at an annealing time of 1 day. Second, ΔH_m shows the opposite trend and decreases with lower temperature. Third, ΔH_m increases with longer annealing time at constant temperature, except for experiments No. 1A and B (Table 1). The highest T_m, around 232 °C, and the highest ΔH_m values (up to 157 Jg^{-1}) were observed at 180° for polymerizations catalyzed by SnBiph but not for those catalyzed by DSTL. Such high values were never reported in the literature for PGAs prepared by ring-opening polymerization. Yet, a T_m of 232 °C and ΔH_m values above 150 Jg^{-1} we were reported in one publication[21] dealing with solid state polycondensation of PGA at temperatures around 190 and 195 °C. Hence, the results of this work and

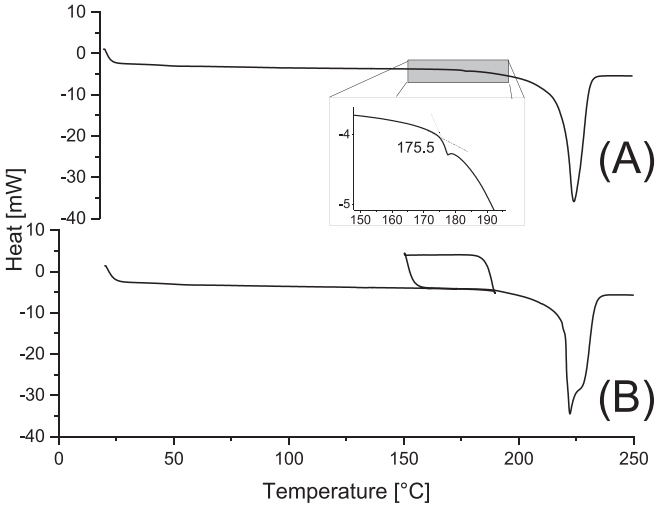

Fig. 6. DSC heating curves of a PGA prepared with DSTL at 160 °C/ 4d (3B, Table 1): (A) first heat (B) heated to 190 °C, cooled to 150 °C and reheated to 250 °C.

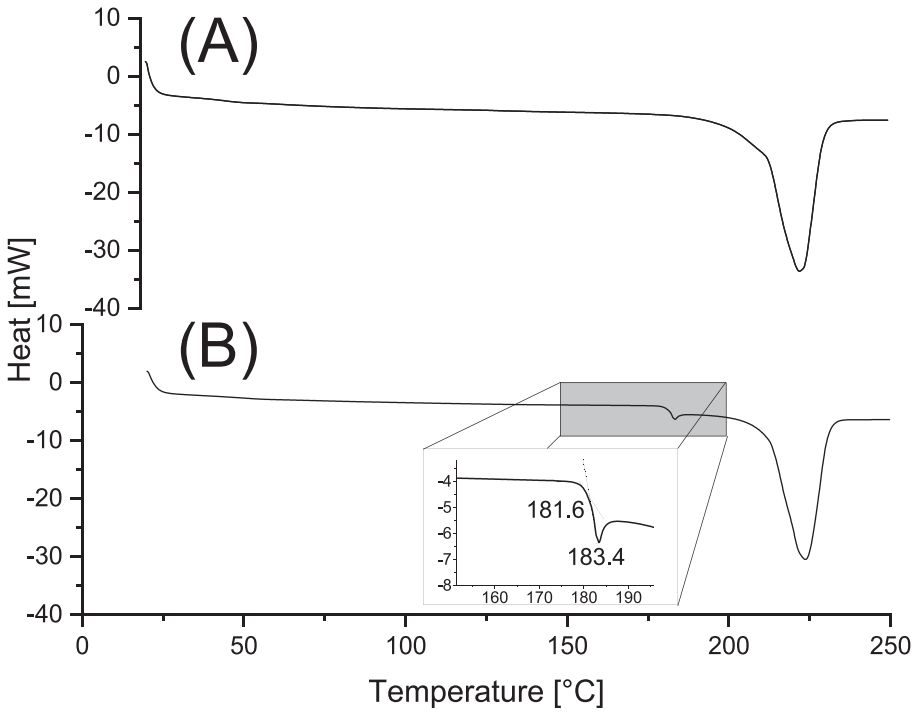

Fig. 7. DSC heating traces of PGAs prepared with SnBiph at 160 °C: (A) after 1 d (3A, Table 2), (B) after 4 d (3B, Table 2).

those of the cited literature indicate that a significant influence of annealing on T_m and ΔH_m may only be expected at temperatures around 180 °C and above.

A quite unexpected phenomenon was observed for sample annealed at 140 or 160 °C for 4 d. A glass transition step became detectable in the range of 170–185 °C. With DSTL as catalyst, this T_g step was extremely weak and only detectable for samples prepared with GA/Cat ratio of 100/1 but not with 500/1 (Fig. 6). These observations suggest that slow transesterification processes are involved in the formation of the phase responsible for these high T_g's. In the case of the more reactive polymerization catalyst SnBiph the high temperature T_g was observable even at a GA/Cat ratio of 500/1, but again an annealing time of 4d was required. The best example of a DSC curve displaying a glass transition around 180 °C was obtained upon annealing at 160 °C (Fig. 7). This glass transition is not detectable, when the PGA samples were annealed at 180 °C and they disappeared upon eating to 190 °C followed immediate cooling and reheating with heating/cooling rates of +/-10 K min^{-1} as usual (Fig. 6B). In other words, the phase responsible for the high temperature T_g is the consequence of a slow thermodynamically controlled process, which is not formed upon rapid heating.

The only hypothesis explaining this phenomenon the authors can offer at this time concerns the relatively immobile disordered ring segments (loops) on both sides of the crystallites. These ring segments possibly adopt a dense antiparallel packing similar to the crystalline phase but with sufficient conformational disorder, so that the X-rays do not identify them as 3d-ordered phase. The mobilization of these conformationally disordered pseudo-crystallites occurs at temperatures just prior to the melting of the less perfect PGA crystals. It should be noted that the formation of this unusual glass transition was also observed for PGAs prepared with other catalysts (as will be reported in a future publication). This indicates that this phenomenon is independent of the polymerization mechanism and catalyst.

3.4. SAXS measurements

It is important to note that SAXS measurements for PGA are extremely rare. Only one long-distance (L) value of PGA prepared by polymerization of glycolide was found in the literature of SAXS measurements for PGA. This value (7.2 nm) agrees well with the L-values found in this work. The SAXS measurements of the DSTL catalyzed PLAs listed in Table 1 gave values that, surprisingly, did not vary with the reaction conditions. Regardless of sample annealing at 140 or 180 °C, and regardless of applied time of 1 d or 4 d, the L- and l_c values were almost constant. In contrast. The L-values of poly(L-lactide)s may vary over broad range (21–40 nm) depending on the reaction conditions and on the thermal history. Typical examples of such SAXS curves are presented in Fig. 8. They display a second order reflection, which indicates a high degree of 3-dimensional order of the crystallites inside the spherulites. Weak trends were detectable, when SnBiph was used as catalyst. Annealing at 180 or at 200 °C had the consequence that the L-values slightly increased, but the l_c values slightly decreased at 200 °C due to decreasing crystallinity, possibly a consequence of thermal degradation. At 180 °C, longer annealing slightly enhanced both crystallinity and crystal thickness as expected. However, even under these harsh conditions the highest L-values did not exceed 8 nm significantly (No. 1A and B, Table 2).

4. Conclusions

The results of the present work suggest the following conclusions. Firstly, both catalysts, DSTL and SnBiph, enable rapid REP of glycolide and yield low and extremely high molar weight cyclic PGA. Secondly, these PGAs display a "saw-tooth pattern" in their mass spectra, indicating the formation of extended-ring crystallites in the mass range below *m/z* 2 500. Thirdly, upon annealing at 160 °C, a high temperature glass-transition is detectable 140 °C above the normal glass transition. Further studies are needed to understand the origin of this glass-transition. Fourth, the DSC measurements prove that crystallinities up to 70 % can be reached after annealing. Fifth, the SAXS measurements indicate that the thickness of the crystallites is rather insensitive to variations of the thermal history. In summary, these experiments yielded a bundle of results that were not predictable from the data published for linear PGAs so far.

Declaration of Generative AI and AI-assisted technologies in the

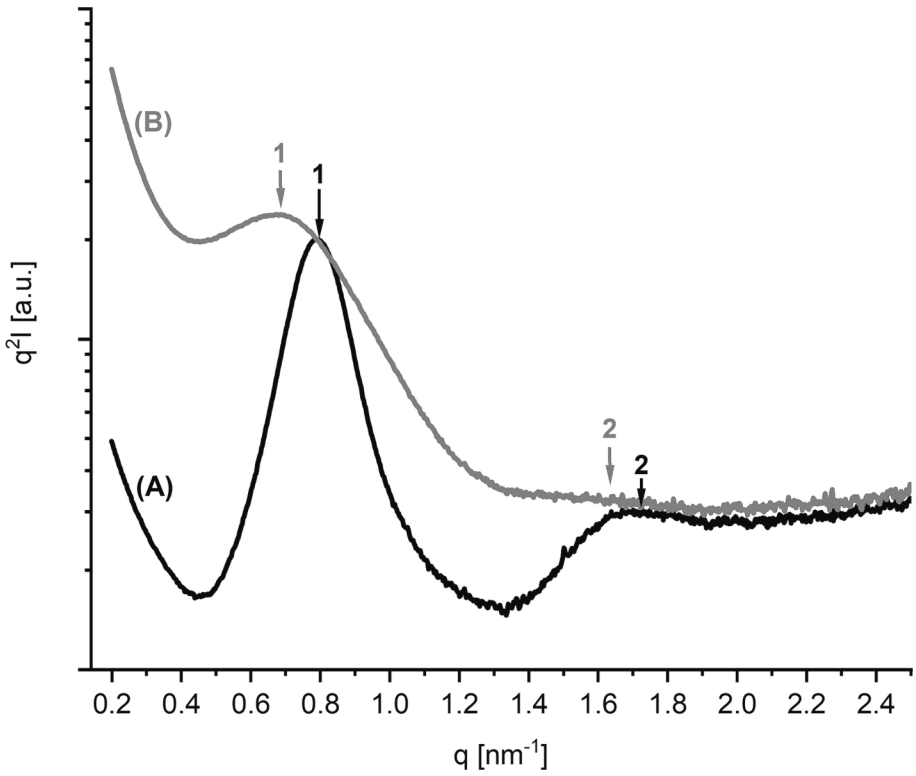

Fig. 8. SAXS curves of PGAs prepared with SnBiph: (A) at 180 °C/3 d (2B, Table 2), (B) at 140 °C/1 d (4A, Table 2).

writing process.

During the preparation of this work the author(s) did not use any AI and AI-assisted technology in the writing process.

CRediT authorship contribution statement

Steffen M. Weidner: Writing – review & editing, Visualization, Methodology, Investigation. **Andreas Meyer:** Visualization, Investigation. **Hans R. Kricheldorf:** Writing – original draft, Methodology, Investigation, Conceptualization.

Declaration of competing interest

The authors declare that they have no known competing financial interests or personal relationships that could have appeared to influence the work reported in this paper.

Data availability

Data will be made available on request.

Acknowledgements

We would like to thank the Bundesanstalt für Materialforschung und -prüfung (BAM) for technical support.

Appendix A. Supplementary data

Supplementary data to this article can be found online at https://doi.org/10.1016/j.eurpolymj.2024.112811.

References

[1] M.L. Beck, US 2 585 427, in: A. Cyanamide (Ed.) US, 1952.
[2] C.E. Lowe, US 2 668 162, in: DuPont (Ed.) US, 1954.
[3] N.A. Higgins, US 2 767 945, in: DuPont (Ed.) US, 1954.
[4] Y. Ishida, H. Ito, M. Takayanagi, Dielectric and viscoelastic behaviors of poly (hydroxyacetic ester), J. Polym. Sci., Part B: Polym. Lett. 3 (2) (1965) 87–94.
[5] K. Chujo, H. Kobayashi, J. Suzuki, S. Tokuhara, Physical and chemical characteristics polyglycolide, Die Makromolekulare Chemie. 100 (1) (1967) 267–270.
[6] Y. Chatani, K. Suehiro, Y. Ôkita, H. Tadokoro, K. Chujo, Structural studies of polyesters. i. crystal structure of polyglycolide, Die, Makromolekulare Chemie. 113 (1) (1968) 215–229.
[7] E.E. Schmitt, M. Epstein, R.A. Polistina, US, 1969. US 3 422 871,.
[8] E.E. Schmitt, US 3 737 440, in: A. Cyanamide (Ed.) US, 1973.
[9] E. Frazza, E. Schmitt, A new absorbable suture, J Biomed Mater Res 5 (2) (1971) 43–58.
[10] D. Gilding, A. Reed, Biodegradable polymers for use in surgery—polyglycolic/poly (actic acid) homo-and copolymers: 1, Polymer. 20 (12) (1979) 1459–1464.
[11] C. Chu, Differential scanning calorimetric study of the crystallization kinetics of polyglycolic acid at high undercooling, Polymer. 21 (12) (1980) 1480–1482.
[12] G. Kister, G. Cassanas, M. Vert, Morphology of poly (glycolic acid) by IR and Raman spectroscopies, Spectrochim. Acta A Mol. Biomol. Spectrosc. 53 (9) (1997) 1399–1403.
[13] P. Dobrzynski, J. Kasperczyk, M. Bero, Application of calcium acetylacetonate to the polymerization of glycolide and copolymerization of glycolide with epsilon-caprolactone and l-lactide, Macromolecules. 32 (14) (1999) 4735–4737.
[14] H. Amine, O. Karima, B.M. El Amine, M. Belbachir, R. Meghabar, Cationic ring opening polymerization of glycolide catalysed by a montmorillonite clay catalyst, J Polym Res. 12 (2005) 361–365.
[15] L.I. Ramdhanie, S.R. Aubuchon, E.D. Boland, D.C. Knapp, C.P. Barnes, D. G. Simpson, G.E. Wnek, G.L. Bowlin, Thermal and mechanical characterization of electrospun blends of poly (lactic acid) and poly (glycolic acid), Polym J. 38 (11) (2006) 1137–1145.
[16] S. Shawe, F. Buchanan, E. Harkin-Jones, D. Farrar, A study on the rate of degradation of the bioabsorbable polymer polyglycolic acid (PGA), J Mater Sci. 41 (2006) 4832–4838.
[17] E. Gautier, P. Fuertes, P. Cassagnau, J.P. Pascault, E. Fleury, Synthesis and rheology of biodegradable poly (glycolic acid) prepared by melt ring-opening polymerization of glycolide, J. Polym. Sci. A Polym. Chem. 47 (5) (2009) 1440–1449.
[18] C. Schmidt, M. Behl, A. Lendlein, S. Beuermann, Synthesis of high molecular weight polyglycolide in supercritical carbon dioxide, Rsc Adv. 4 (66) (2014) 35099–35105.
[19] R.R. Nakka, V.R. Thumu, R.R. SVS, S.R. Buddhiraju, The study of gamma irradiation effects on poly (glycolic acid), Radiat Eff. Defects Solids 170 (5) (2015) 439–450.
[20] C. Yu, J. Bao, Q. Xie, G. Shan, Y. Bao, P. Pan, Crystallization behavior and crystalline structural changes of poly (glycolic acid) investigated via temperature-variable WAXD and FTIR analysis, CrstEngComm. 18 (40) (2016) 7894–7902.

[21] M. Ayyoob, D.H. Lee, J.H. Kim, S.W. Nam, Y.J. Kim, Synthesis of poly (glycolic acids) via solution polycondensation and investigation of their thermal degradation behaviors, Fibers Polym. 18 (2017) 407–415.
[22] V. Sanko, I. Sahin, U. Aydemir Sezer, S. Sezer, A versatile method for the synthesis of poly (glycolic acid): high solubility and tunable molecular weights, Polym J. 51 (7) (2019) 637–647.
[23] K. Chen, S.L. Yang, Preparation of high-molecular-weight poly(glycolic acid) by direct melt polycondensation from glycolic acid, Adv. Mat. Res. 821 (2013) 1023–1026.
[24] A. Pinkus, R. Subramanyam, New high-yield, one-step synthesis of polyglycolide from haloacetic acids, J. Polym. Sci., Polym. Chem. Ed. 22 (5) (1984) 1131–1140.
[25] K. Schwarz, M. Epple, A detailed characterization of polyglycolide prepared by solid-state polycondensation reaction, Macromol Chem Physic. 200 (10) (1999) 2221–2229.
[26] O. Herzberg, R. Gehrke, M. Epple, Combined in-situ small and wide-angle synchrotron X-ray scattering (SAXS-WAXS) applied to a solid-state polymerization reaction, Polymer. 40 (2) (1999) 507–511.
[27] K. Takahashi, I. Taniguchi, M. Miyamoto, Y. Kimura, Melt/solid polycondensation of glycolic acid to obtain high-molecular-weight poly (glycolic acid), Polymer. 41 (24) (2000) 8725–8728.
[28] E. Göktürk, A.G. Pemba, S.A. Miller, Polyglycolic acid from the direct polymerization of renewable C1 feedstocks, Polym Chem-Uk 6 (21) (2015) 3918–3925.
[29] H.R. Kricheldorf, S. Weidner, F. Scheliga, Cyclic poly (L-lactide)s via ring-expansion polymerizations catalysed by 2, 2-dibutyl-2-stanna-1, 3-dithiolane, Polym Chem-Uk. 8 (9) (2017) 1589–1596.
[30] H.R. Kricheldorf, S.M. Weidner, High molar mass cyclic poly (L-lactide) via ring-expansion polymerization with cyclic dibutyltin bisphenoxides, Eur. Polym. J. 105 (2018) 158–166.
[31] S.M. Weidner, A. Meyer, S. Chatti, H.R. Kricheldorf, About the transformation of low T-m into high T-m poly(l-lactide)s by annealing under the influence of transesterification catalysts, Rsc Adv. 11 (5) (2021) 2872–2883.
[32] H.R. Kricheldorf, S.M. Weidner, A. Meyer, Poly(l-lactide): optimization of melting temperature and melting enthalpy and a comparison of linear and cyclic species, Materials Advances. 3 (2) (2022) 1007–1016.
[33] H.R. Kricheldorf, S.M. Weidner, A. Meyer, Ring-expansion polymerization (REP) of L-lactide with cyclic tin catalysts–About formation of extended ring crystals and optimization of Tm and ΔHm, Polymer. 263 (2022) 125516.
[34] H.R. Kricheldorf, S.M. Weidner, A. Meyer, About the Influence of (Non-) solvents on the ring expansion polymerization of l-lactide and the formation of extended ring crystals, Macromol Chem Physic. 224 (5) (2023) 2200385.
[35] H.R. Kricheldorf, S.M. Weidner, F. Scheliga, Cyclic polylactides via simultaneous ring-opening polymerization and polycondensation catalyzed by dibutyltin mercaptides, J. Polym. Sci. A Polym. Chem. 55 (22) (2017) 3767–3775.
[36] G. Benecke, W. Wagermaier, C. Li, M. Schwartzkopf, G. Flucke, R. Hoerth, I. Zizak, M. Burghammer, E. Metwalli, P. Müller-Buschbaum, A customizable software for fast reduction and analysis of large X-ray scattering data sets: Applications of the new DPDAK package to small-angle X-ray scattering and grazing-incidence small-angle X-ray scattering, J. Appl. Cryst. 47 (5) (2014) 1797–1803.
[37] L. Lu, A.G. Mikas, Polyglycolic Acid, in: J.E. Mark (Ed.), Polymer Data Handbook, Oxford University Press, Oxford/New York, 1999, pp. 566–569.
[38] H.R. Kricheldorf, S.M. Weidner, A. Meyer, High T_m linear poly(l-lactide)s prepared via alcohol-initiated ROPs of l-lactide, Rsc Adv. 11 (23) (2021) 14093–14102.
[39] H. Kricheldorf, S.M. Weidner, F. Scheliga, Ring-expansion polymerization (REP) of l-lactide with cyclic tin(II) bisphenoxides, Eur. Polym. J. 116 (2019) 256–264.
[40] S.M. Weidner, A. Meyer, J. Falkenhagen, H.R. Kricheldorf, $SnOct_2$-catalyzed and alcohol-initiated ROPs of L-lactide–about the influence of initiators on chemical reactions in the melt and the solid state, Eur. Polym. J. 153 (2021) 110508.
[41] H.R. Kricheldorf, S.M. Weidner, Cyclic poly (L-lactide)s via simultaneous ROP and polycondensation (ROPPOC) catalyzed by dibutyltin phenoxides, Eur. Polym. J. 109 (2018) 360–366.
[42] H. Hirono, G. Wasai, T. Mitsueda, J. Furukawa, Journal of the Chemical Society of Japan, Chemistry and Industrial Chemistry 67 (1964) 604–606.
[43] S.M. Weidner, A. Meyer, H. Kricheldorf, Sn(II)2-ethylhexanoate-catalyzed polymerizations of l-lactide in solution – Solution grown crystals of cyclic Poly(l-Lactide)s, Polymer. 255 (2022) 125142.
[44] H.R. Kricheldorf, S.M. Weidner, About the crystallization of cyclic and linear poly (L-lactide)s in alcohol-initiated and Sn (II) 2-ethylhexanoate-catalyzed ROPs of L-lactide conducted in solution, Polymer. 276 (2023) 125946.